ELSEVIER

Journal of Alloys and Compounds 434–435 (2007) 71–74

Journal of ALLOYS AND COMPOUNDS

www.elsevier.com/locate/jallcom

Thermal and mechanical properties of Cu–Zr–Al bulk metallic glasses

T.L. Cheung, C.H. Shek *

Department of Physics and Materials Science, City University of Hong Kong, Tat Chee Avenue, Kowloon Tong, Hong Kong, China

Available online 13 October 2006

Abstract

The effects of adding small amount of aluminum to the binary $Cu_{50}Zr_{50}$ bulk metallic glass (BMG) on the thermal and mechanical properties were investigated. The Al addition was limited to $3 \leq x \leq 10$ at.% in order to form fully amorphous bulk samples. Glassy rods of 3 mm diameter of these alloys were prepared by copper mold suction casting. The $(Cu_{50}Zr_{50})_{100-x}Al_x$ BMGs ($x = 0$ and $3 \leq x \leq 10$ at.%) were characterized with differential scanning calorimetry (DSC), X-ray diffraction (XRD), Vickers microhardness test and nanoindentation, respectively. The glass transition temperatures, crystallization temperatures and super-cooled liquid regions of the specimens increased with increasing Al content. The microhardness of the specimens also increases with increasing Al content. Room temperature nanoindentation was carried out on the cross-section of the rods. The results showed that the nanohardness and creep displacement were dependent on the Al content.

Keywords: Metallic glasses; Mechanical properties; Thermal analysis; X-ray diffraction

1. Introduction

In recent years, researchers are interested in developing bulk metallic glasses which exhibits high glass forming abilities (GFAs) along with good mechanical properties. Inoue et al. reported the formation of Cu-based BMGs with high tensile strength of over 2000 MPa and good ductility [1–3]. Most of the Cu-based BMGs are formed from much cheaper materials than those used in other BMG families such as Zr-, Ti- and Ni-based BMGs. The Cu–Zr–Al BMGs, among different Cu-based systems, were found exhibiting all the above advantages. Formation of alloy having high GFA with inexpensive materials is not only of scientific interest but make the production of precision mechanical parts possible as well [4].

Binary BMG such as Cu–Zr glassy alloy attracted a lot of attention in the past few years due to its simple constituents [5–10]. The Cu–Zr binary BMG exhibits high strength [5,6,8,10], reasonable plasticity [7], high glass transition temperature and wide super-cooled liquid region [5,7–10]. However, binary Cu–Zr BMGs usually contain fine crystals of nanometer scale which slightly reduce the strength [7,8]. Previous studies confirmed that suitable addition of a small amount of a third element can suppress the nucleation of crystals and hence, improve the GFA of the alloys effectively [8,11–15]. In this investigation, small amount of Al was added to the $Cu_{50}Zr_{50}$ alloy and the effects on GFA and hardness were studied. Owing to the high hardness and reasonable toughness of BMGs, it is worthwhile to explore its mechanical properties for better functional applications in the products. The nanoindenter was commonly used to measure the hardness (H) and modulus (E) as well as shear band activities of BMGs. Besides, the nanoindenter can be used to study the localized nanoindentation creep by impression creep test [16]. In this paper, the mechanical properties including creep behavior of $(Cu_{50}Zr_{50})_{100-x}Al_x$ BMGs with different Al content were studied using nanoindenter as well as microhardness measurement.

2. Experimental procedure

A series of $(Cu_{50}Zr_{50})_{100-x}Al_x$ ($x = 0$, 3, 4, 6, 7, 8, 10 and 12) alloys were prepared by arc melting the mixtures of Cu, Zr and Al with purities higher than 99.9 (at.%) in a Ti-gettered argon atmosphere. The BMG samples were produced by suction casting into a copper mold to form 3 mm diameter and 50 mm long rods. The amorphous structure was checked with a Siemens D500 diffractometer with Cu Kα ($\lambda = 0.1542$ nm) radiation. The thermal properties of the as-cast samples were measured with a Perkin Elmer DSC 7 under a purified nitrogen atmosphere. The DSC was calibrated with the melting transition of indium and zinc prior to data collection. The DSC scan was made from 323 to 873 K at a constant heating rate of 20 K/min. The thermodynamic behavior including the glass transition temperature (T_g) and the onset crystallization temperature (T_x) were found from the DSC curves. Vickers microhardness tests were done on the as-cast samples with a Matsuzawa MXT-α7 digital microhardness tester with

* Corresponding author. Tel.: +852 27887798; fax: +852 27887830.
E-mail address: apchshek@cityu.edu.hk (C.H. Shek).

0925-8388/$ – see front matter © 2006 Elsevier B.V. All rights reserved.
doi:10.1016/j.jallcom.2006.08.109

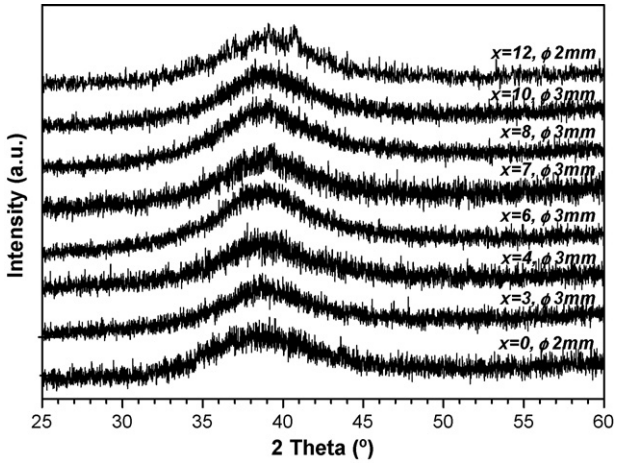

Fig. 1. XRD spectra of the $(Cu_{50}Zr_{50})_{100-x}Al_x$ ($x = 0$, 3, 4, 6, 7, 8, 10 and 12) alloys.

a load of 100 g (0.98 N). The samples were cut into cylinders with thickness of 2 mm and the surfaces were ground flat to parallel before hardness test. Specimens for nanoindentation tests were prepared similar to that for microhardness test but were polishing to a mirror like finish before the test. Nanoindentation test were performed on the as-cast samples with a Nano Indenter® XP for studying the creep behavior while hardness and modulus measurement were made with a CSEM nanohardness tester. Deformation load was applied through a Berkovich triangular diamond indenter in the Nano Indenter® XP driven by an electromagnet. The indentation cycle consisted of a constant loading part up to a maximum load of 200 mN followed by a first hold period of 900 s at the maximum load, the unloading part and a second hold period of 40 s at 10% of the maximum load.

3. Results and discussions

3.1. X-ray diffraction

Fig. 1 shows the XRD spectra of the as-cast 2 mm diameter $Cu_{50}Zr_{50}$ BMG, and other samples, with diffraction angle 2θ from 25° to 60°. The XRD pattern exhibits broad diffuse peak between diffraction angles 30° and 45°, indicating the glassy state of the binary alloy sample. In recent work by Yu et al. [17], the XRD spectrum for 3 mm $Cu_{50}Zr_{50}$ rod exhibits sharp crystalline peaks, which indicated that the metastable crystalline $Cu_{51}Zr_{14}$ phase existed. Besides, Inoue et al. [7] and Das et al. [8] also found that there are tiny crystals present in the glassy matrix. After adding 2 at.% of Al content, crystalline $ZrAl_2$ and other unknown phases formed instead of forming the $Cu_{51}Zr_{14}$ phase [17]. It reveals that the Cu–Zr binary system can no longer be formed in fully amorphous state when the sample diameter exceeds 2 mm.

The X-ray diffraction patterns of the as-cast $(Cu_{50}Zr_{50})_{100-x}Al_x$ rods with 3 mm diameters are also shown in Fig. 1. For $x = 3$, 4, 6, 7, 8 and 10, the spectra only consist of broad diffraction peaks, indicating their glassy state. When $x = 12$, some peaks are detected from the pattern though it shows a broad diffuse background. Those peaks of crystallized phases cannot be indexed unambiguously. The XRD results clearly show that there is a critical Al content for the formation of $(Cu_{50}Zr_{50})_{100-x}Al_x$ BMGs. In order to form fully amorphous structure, the Al content is limited to $3 \le x \le 10$ at.%.

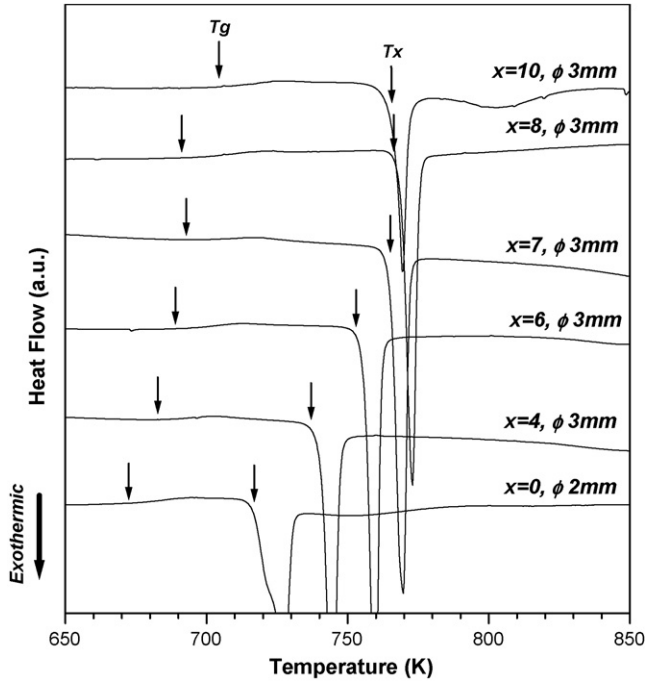

Fig. 2. DSC curves of the $(Cu_{50}Zr_{50})_{100-x}Al_x$ ($x = 0$, 3, 4, 6, 7, 8 and 10) glassy alloys.

3.2. Thermal analysis with DSC

Fig. 2 shows the DSC traces of the as-cast $(Cu_{50}Zr_{50})_{100-x}Al_x$ ($x = 3$, 4, 6, 7, 8 and 10 at.%) glassy alloys in the temperature range from 650 to 850 K. The alloys exhibit distinct glass transitions, followed by super-cooled liquid regions (SLR), and then the exothermic reaction corresponding to crystallization. The glass transition temperatures (T_g), the onset temperatures of crystallization (T_x) and the SLR ($\Delta T_x = T_g - T_x$) are plotted against the Al content in Fig. 3, and the data are also summarized in Table 1.

Both the T_g and T_x increase with increasing Al content. The T_g increases from 673 to 704 K when Al content increases from

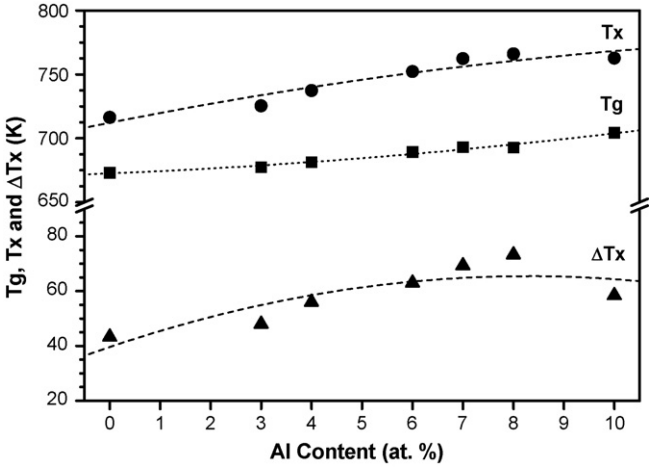

Fig. 3. Variations in the glass transition temperature (T_g), crystallization temperature (T_x) and super-cooled liquid region (ΔT_x) as a function of Al content of the $(Cu_{50}Zr_{50})_{100-x}Al_x$ ($x = 0$, 3, 4, 6, 7, 8 and 10) glassy alloys.

Table 1
Thermal parameters and mechanical properties of $(Cu_{50}Zr_{50})_{100-x}Al_x$ glassy alloys

Composition (at.%)	T_g (K)	T_x (K)	ΔT_x (K)	Vickers microhardness (H_v)	H (GPa)	E (GPa)
Cu50Ar50	673	716	43	449	7.3	100.5
$(Cu_{50}Zr_{50})_{97}Al_3$	677	725	48	477	7.4	103.0
$(Cu_{50}Zr_{50})_{96}Al_4$	681	737	56	489	7.8	107.6
$(Cu_{50}Zr_{50})_{94}Al_6$	689	752	63	506	8.0	109.0
$(Cu_{50}Zr_{50})_{93}Al_7$	693	762	69	521	8.5	111.6
$(Cu_{50}Zr_{50})_{92}Al_8$	692	766	73	526	8.6	115.2
$(Cu_{50}Zr_{50})_{90}Al_{10}$	704	763	58	541	8.7	117.3

0 to 10 at.%, while the T_x increases from 716 to 766 K for Al content of 0–8 at.%. The highest value of ΔT_x, 73 K, is obtained when $x = 8$, which is a relatively large value and indicates that $(Cu_{50}Zr_{50})_{92}Al_8$ has an excellent thermal stability against crystallization. This agrees quite well with the result of Yu et al. [17]. Besides, the ΔT_x increases from 43 to 73 K for Al content of 0–8 at.%. It clearly shows that a small amount of Al addition can improve the thermal stability of this alloy.

3.3. Microhardness measurement

Fig. 4 presents the changes of Vickers microhardness (H_v) with Al content. The data are also summarized in Table 1. The hardness increases almost linearly from 449 to 541 H_v for $x = 0$–10. The substitution of Al in Cu–Zr glassy alloy can effectively increase its mechanical hardness. The experimental error bars in Fig. 5 are below 5%. The minor fluctuation may be attributed to experimental errors during the test, or to some minor compositional fluctuation [18].

3.4. Nanohardness

The nanohardness (H) and elastic modulus (E) as a function of Al content are shown in Fig. 5 and Table 1. The term modulus is used instead of Young's modulus, as it is still not completely confirmed that the conventional Young's modulus can be obtained from every indentation experiment [19]. The H and E increases from 7.3 to 8.3 GPa and from 100 to 117 GPa, respectively, for the increase of x from 0 to 10. The microhardness measured above is relatively smaller than the nanohardness on the same specimen. The major reasons are due to the difference in geometry, size, indentation depth and loading mode of the indenters of the two different tests [18].

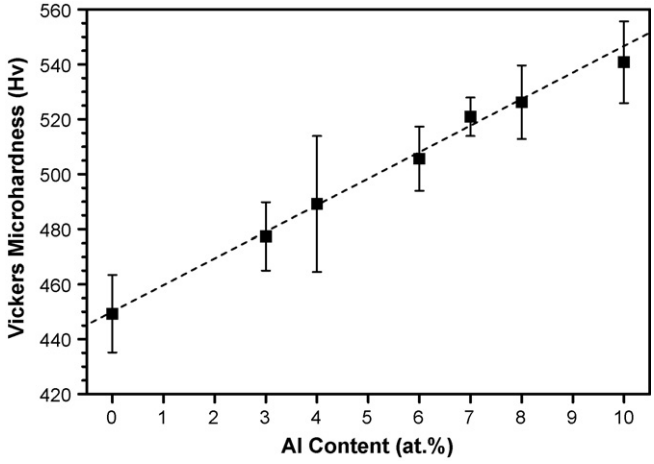

Fig. 4. Microhardness vs. Al content of the $(Cu_{50}Zr_{50})_{100-x}Al_x$ ($x = 0$, 3, 4, 6, 7, 8 and 10) glassy alloys.

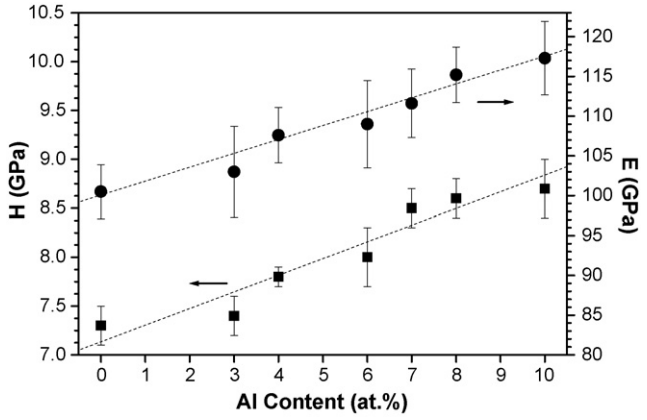

Fig. 5. Nanohardness vs. Al content of the $(Cu_{50}Zr_{50})_{100-x}Al_x$ ($x = 0$, 3, 4, 6, 7, 8 and 10) glassy alloys.

3.5. Creep behavior

Fig. 6 shows that the result of displacement versus time curves of the $(Cu_{50}Zr_{50})_{90}Al_{10}$ glassy alloy measured with a Nano Indenter® XP. The corresponding load/unload profile is also shown in the same figure for reference. After holding the load for 900 s at the maximum load of 200 mN, a positive creep behavior

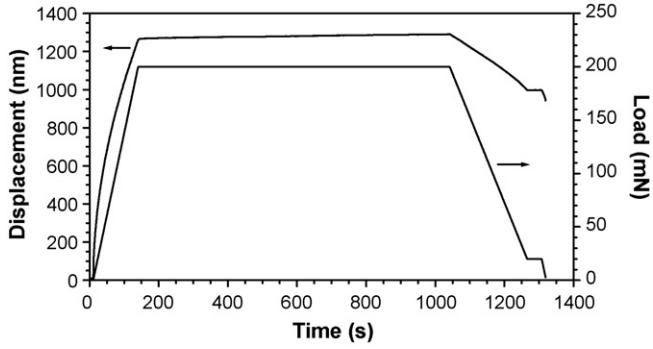

Fig. 6. Displacement vs. time graph during holding at peak load by nanoindentation test on $(Cu_{50}Zr_{50})_{90}Al_{10}$ glassy alloy.

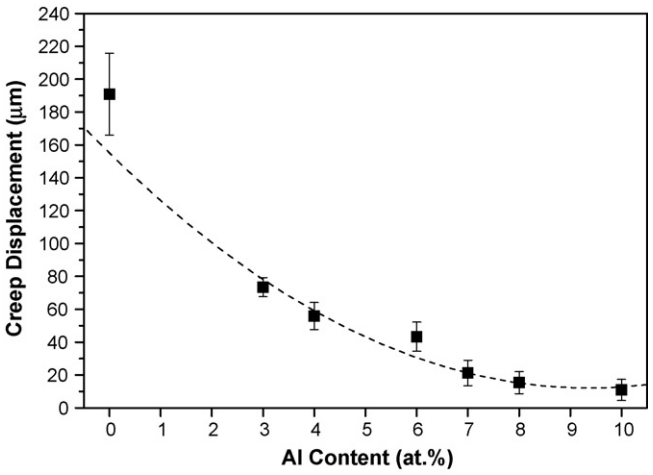

Fig. 7. Creep displacement vs. Al content during holding at peak load for the $(Cu_{50}Zr_{50})_{100-x}Al_x$ ($x = 0$, 3, 4, 6, 7, 8 and 10) glassy alloys.

is observed in the $(Cu_{50}Zr_{50})_{100-x}Al_x$ metallic glass. The creep displacement versus Al content curve is shown in Fig. 7. The creep displacement decreases from 191 μm for $x = 0$–12 nm for $x = 10$. Creep is closely related to plastic deformation, and hardness is a measure of material's resistance to localized plastic deformation. Thus creep has a close relationship with mechanical strength. From the above results, the hardness increases with increasing Al content, in contrast, the creep displacement decreases with increasing Al content. This shows that the trend of creep behavior is in line with the trend of the hardness.

4. Conclusions

The influences of adding a minor Al content to the Cu–Zr glassy alloys can improve the thermal stability, mechanical properties and GFA. When 8 at.% of Al content is added, the ΔT_x is optimized at 73 K and the alloy has the highest thermal stability among the series of samples. The hardness was enhanced to 541 H_v by adding 10 at.% of Al. Due to the close relationship between creep and hardness, the creep displacement is the largest for the $Cu_{50}Zr_{50}$ bulk glassy alloy and thus the smallest for $(Cu_{50}Zr_{50})_{90}Al_{10}$ glassy alloy.

Acknowledgements

The authors would like to express their gratitude to Professor W.H. Wang and Mr. D.Q. Zhao, Institute of Physics, Chinese Academy of Sciences, for their support in the preparation of the bulk metallic glass samples. I would like to express my special thanks to Dr. A.H.W. Ngan for kindly providing the Nano Indenter CSEM and his assistance in the nanoindentation experiments. This work is supported by a City University of Hong Kong Research Grant (Grant number: 7001773).

References

[1] A. Inoue, W. Zhang, K. Kuroaska, J. Non-Cryst. Solids 304 (2002) 200–209.
[2] A. Inoue, W. Zhang, T. Zhang, K. Kuroaska, Acta Mater. 49 (2001) 2645–2652.
[3] A. Inoue, W. Zhang, Mater. Trans. 43 (11) (2002) 2921–2925.
[4] T. Masumoto, Mater. Sci. Eng. A 179/180 (1994) 8–16.
[5] Z.W. Zhu, H.F. Zhang, W.S. Sun, B.Z. Ding, Z.Q. Hu, Scr. Mater. 54 (2006) 1145–1149.
[6] D.C. Hofmann, G. Duan, W.L. Johnson, Scr. Mater. 54 (2006) 1117–1122.
[7] A. Inoue, W. Zhang, T. Tsurui, A.R. Yavari, A.L. Greer, Philos. Mag. Lett. 85 (2005) 221–229.
[8] J. Das, M.B. Tang, K.B. Kim, R. Theissmann, F. Baier, W.H. Wang, J. Eckert, Phys. Rev. Lett. 94 (2005) 205501-1–1205501-3.
[9] M.B. Tang, D.Q. Zhao, M.X. Pan, W.H. Wang, Chin. Phys. Lett. 21 (2004) 901–903.
[10] D.H. Xu, B. Lohwongwatana, G. Duan, W.L. Johnson, C. Garland, Acta. Mater. 52 (2004) 2621–2624.
[11] W.H. Wang, Q. Wei, H.Y. Bai, Appl. Phys. Lett. 71 (1997) 58–60.
[12] W.H. Wang, Z. Bian, P. Wen, Y. Zhang, M.X. Pan, D.Q. Zhao, Intermetallics 10 (2002) 1249–1257.
[13] Y. Zhang, M.X. Pan, D.Q. Zhao, R.J. Wang, W.H. Wang, Mater. Trans. 41 (2000) 1410–1414.
[14] Z.P. Lu, C.T. Liu, Appl. Phys. Lett. 83 (2003) 2581–2583.
[15] A. Inoue, T. Zhang, H. Koshiba, J. Appl. Phys. 83 (1998) 6326–6328.
[16] S. Chu, J.C.M. Li, J. Mater. Sci. 12 (1977) 2200.
[17] P. Yu, H.Y. Bai, M.B. Tang, W.L. Wang, J. Non-Cryst. Solids 351 (2005) 1328–1332.
[18] H. Zhang, G. Subhash, L.J. Kecskes, R.J. Dowding, Scr. Mater. 49 (2003) 447–452.
[19] T. Chudoba, F. Richter, Surf. Coat. Technol. 148 (2001) 191–198.